THE JOURNAL OF PHYSICAL CHEMISTRY C

Article

pubs.acs.org/JPCC

Catalytic Hydrogenation and Hydrodeoxygenation of Furfural over Pt(111): A Model System for the Rational Design and Operation of Practical Biomass Conversion Catalysts

Martin J. Taylor,[†,‡] Li Jiang,[§] Joachim Reichert,[§] Anthoula C. Papageorgiou,[§] Simon K. Beaumont,[∥] Karen Wilson,[†] Adam F. Lee,[†] Johannes V. Barth,[§] and Georgios Kyriakou*[,†,‡]

[†]European Bioenergy Research Institute, Aston University, Aston Triangle, Birmingham B4 7ET, United Kingdom

[‡]Chemical Engineering and Applied Chemistry, Aston University, Aston Triangle, Birmingham B4 7ET, United Kingdom

[§]Physik-Department E20, Technische Universität München, D-85748 Garching, Germany

[∥]Department of Chemistry, Durham University, South Road, Durham DH1 3LE, United Kingdom

Supporting Information

ABSTRACT: Furfural is a key bioderived platform chemical whose reactivity under hydrogen atmospheres affords diverse chemical intermediates. Here, temperature-programmed reaction spectrometry and complementary scanning tunneling microscopy (STM) are employed to investigate furfural adsorption and reactivity over a Pt(111) model catalyst. Furfural decarbonylation to furan is highly sensitive to reaction conditions, in particular, surface crowding and associated changes in the adsorption geometry: furfural adopts a planar geometry on clean Pt(111) at low coverage, tilting at higher coverage to form a densely packed furfural adlayer. This switch in adsorption geometry strongly influences product selectivity. STM reveals the formation of hydrogen-bonded networks for planar furfural, which favor decarbonylation on clean Pt(111) and hydrogenolysis in the presence of coadsorbed hydrogen. Preadsorbed hydrogen promotes furfural hydrogenation to furfuryl alcohol and its subsequent hydrogenolysis to methyl furan, while suppressing residual surface carbon. Furfural chemistry over Pt is markedly different from that over Pd, with weaker adsorption over the former affording a simpler product distribution than the latter; Pd catalyzes a wider range of chemistry, including ring-opening to form propene. Insight into the role of molecular orientation in controlling product selectivity will guide the design and operation of more selective and stable Pt catalysts for furfural hydrogenation.

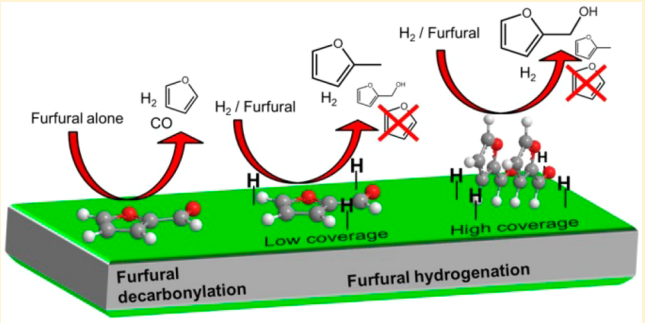

INTRODUCTION

The development and sustainability of a bioresource-based chemical industry is strongly dependent on new heterogeneously catalyzed processes capable of selectively transforming bioderived organic molecules into valuable chemical intermediates, platform chemicals, and commercial products. In this respect, fundamental understanding of the underlying mechanistic aspects governing these heterogeneous processes is crucial. Lignocellulosic and oleochemical biomass-derived molecules are most attractive because of their abundance and the plethora of products that can be derived from them. Furfural is one of the most promising renewable platform compounds,[1−4] itself obtainable via the acid-catalyzed hydrolysis of C5 sugars such as xylans and xylose.[3,5]

Furfural can be upgraded for a range of applications, finding use as a process agent for generating lubricating oils and in the flavorings and perfume industry where subtle structural alterations unlock diverse flavorings.[3] However, the majority of furfural (>62%) is hydrogenated to furfuryl alcohol for use as an adhesive, resin, or corrosion-resistant coating.[2,6] Furfuryl alcohol is also a chemical building block to many other useful compounds in the fine chemical and pharmaceutical industries, as shown in Scheme 1,[7] offering a route to 2-methyl furan, a potential biofuel, or tetrahydrofurfuryl alcohol (B) which can in turn undergo ring-opening hydrogenation to the polymer precursor 1,5-pentandiol (D).[8] While 2-methyl furan production is reported for Pd hydrogenolysis catalysts in the liquid phase,[9,10] it is observed only at high temperature over Pt.[11−15]

Large-scale furfural upgrading already occurs in China, South Africa, and the Dominican Republic, utilizing ∼280 000 tons of furfural per annum.[1] However, current processes rely on a copper chromite catalyst which damages both ecologies and human health.[16,17] This copper chromite catalyst operates at high pressure (up to 30 bar) and high temperature (up to 473

Received: February 23, 2017
Revised: March 28, 2017
Published: March 28, 2017

DOI: 10.1021/acs.jpcc.7b01744
J. Phys. Chem. C 2017, 121, 8490−8497

Scheme 1. Furfural and Its Derivatives: (A) Tetrahydrofuran, (B) Tetrahydrofurfuryl Alcohol, (C) 1,2-Pentanediol, and (D) 1,5-Pentanediol

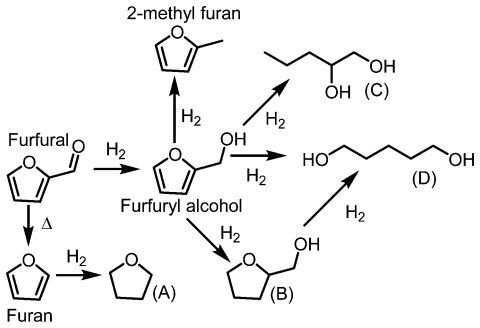

K), affording acceptable selectivity and reasonable activity, but in light of its associated hazards, a replacement catalyst is urgently sought (especially if the transition from a petrochemical to biobased economy proceeds apace).[2,18]

Furfural hydrogenation has been studied in both the vapor and liquid phase[11,19−23] and is highly sensitive to reaction conditions over Pt catalysts. In general, liquid-phase hydrogenation is conducted at lower temperature than vapor-phase studies, hindering direct comparison because of the widely differing product distributions.

Higher temperature favors ring-opening or total hydrogenation of furfural, while mild conditions favor furfuryl alcohol and furan.[11,20,24] Liquid-phase hydrogenation is complicated by poor hydrogen solubility in the reaction medium and competitive solvent coupling reactions to form 1° and 2° alcohols (prolific in furfural chemistry);[11,12,14] hence, high hydrogen pressures are common. Vapor-phase studies require temperature only >435 K to vaporize furfural at atmospheric pressure.[25] However, the key factors determining product selectivity and activity are not well-established. Many transition-metal catalysts are reported for the hydrogenation of furfural to furfuryl alcohol, including Ni, Pd, Co, Cu, Rh, Ir, and Ru.[13,22,23,26−29] Platinum has been particularly explored under mild reaction conditions,[11] for vapor-phase hydrogenation, with high reaction temperatures yielding a spectrum of small molecules including methyl furan.[20,30] In contrast, over Pd, an array of products forms during liquid-phase furfural hydrogenation,[10] such as acetals, ketals, and polymeric species, in addition to ring-opening products.[31]

Adsorption of unsaturated oxygenates over Cu, Ni, Pd, and Pt(111) single-crystal surfaces and Zn adatom modified Pt(111)[32−45] has been the focus of both experimental and theoretical investigations. For furfural, reactively formed furan (a decarbonylation product from furfural and furfuryl alcohol) behaves differently from molecular furan over Pd(111), the former being more prone to thermal decomposition to propylene.[39,46] Density functional theory (DFT) calculations have highlighted multiple reaction pathways for furfuryl alcohol hydrogenolysis over Pd(111) accompanied by the formation of adsorbed water; calculations suggest that the latter byproduct hinders furfural hydrogenation over Cu(111).[32] Furfural adsorption and decomposition over Pt(111) and Zn-modified Pt(111) have been extensively investigated using temperature-programmed desorption (TPD) and high-resolution electron energy loss spectroscopy by Shi and Vohs.[38] They report that furfural adsorbs at low temperatures through the aromatic ring on Pt(111) driving unselective decomposition to CO and H_2 upon heating. Surface modification with Zn adatoms favors furfural adsorption through the carbonyl carbon and associated ring tilting away from the Pt(111) surface.[38] This molecular reorientation suppresses thermal decomposition and ring hydrogenation in favor of hydrodeoxygenation (HDO) of the C═O bond.

Here we utilize temperature-programmed reaction spectrometry (TPRS) and scanning tunneling microscopy (STM) to elucidate salient features of furfural's adsorption and hydrogenation over Pt(111) and correlate coverage-dependent orientation and self-assembly with selectivity toward hydrogenation versus decomposition pathways. Furfural adsorbs in a hydrogen-bonded planar network at low coverage, adopting a tilted geometry for a densely packed furfural adlayer. Adsorption geometry and hydrogen coadsorption influence selectivity toward both evolved products and surface carbon. Preadsorbed hydrogen promotes hydrogenation to furfuryl alcohol over decarbonylation to furan and passivates Pt(111) toward molecular decomposition. These results specifically allow us to discuss the fundamental surface behavior of furfural that leads to the selectivity of platinum versus other precious metal catalysts, such as palladium, in this important hydrogenation reaction. They also identify the critical importance of surface hydrogen concentration in both selectivity and deactivation as a result of surface coking by carbon. In consequence, the present findings help pave the way toward replacement catalysts for the undesirable copper chromite catalyst packages currently employed.

■ EXPERIMENTAL SECTION

TPRS was conducted in an ultrahigh vacuum (UHV) chamber operated at a base pressure of 3×10^{-10} Torr, equipped with an Omicron 4 grid retarding field analyzer for low-energy electron diffraction (LEED) or Auger electron spectroscopy (AES) and a VG 300 quadrupole mass spectrometer whose ionizer was positioned 6 mm from the front face of the sample. The Pt(111) single crystal could be cooled to 140 K and resistively heated to above 1000 K, monitored by a K-type thermocouple attached to the sample. Furfural (Sigma-Aldrich, 99%), furan (Sigma-Aldrich, ≥ 99%), 2-methyl furan (Sigma-Aldrich, 99%), and furfuryl alcohol (Sigma-Aldrich, 98%) were purified by several freeze−pump−thaw cycles. All organic molecules, H_2 (Energas, 99.99%), and O_2 (Energas, 99.999%) were delivered to the sample by backfilling the chamber to the required pressure. TPD and TPRS measurements were performed with a linear heating ramp of 9.9 K s^{-1}. Selectivity calculations (see the Supporting Information) from the mass spectrometry data include corrections for mass spectrometer sensitivity and molecular ionization cross section achieved by admitting a known pressure of each molecule into the vacuum system, measuring the intensity of the mass fragments, and correcting the pressure gauge reading based on the theoretical ionization cross section. Mass fragments for molecular identification were as follows; furfural (m/z 96 and 39), furan (m/z 68 and 39), furfuryl alcohol (m/z 98, 81, and 39), and methyl furan (m/z 82, 53, and 39). Additional ions were also monitored to identify potential products tetrahydrofuran (m/z 72), tetrahydrofurfuryl alcohol (m/z 102), 2-methyltetrahydrofuran (m/z 82), and propene (m/z 42); however, none of these latter molecules were detected from furfural with and without coadsorbed H_2. Exposures are quoted in Langmuirs (L), where 1 L is 1×10^{-6} Torr s^{-1} and have been corrected for ion gauge sensitivity. STM measurements were carried out in a separate custom built UHV

DOI: 10.1021/acs.jpcc.7b01744
J. Phys. Chem. C 2017, 121, 8490−8497

system (base pressure low 10^{-10} Torr) with a commercial STM Aarhus 150 supplied by SPECS using a chemically etched tungsten tip held at 293 K. Furfural molecules were dosed in situ. The tunneling bias (V_t) is applied to the sample. STM micrographs were processed using the WSxM software[47] by adjustment of the plane and contrast and appropriate application of moderate Gaussian smoothing. Quoted coverages are based on estimation of the monolayer point (1 monolayer = 1 ML) from the appearance of a multilayer peak in the TPD data and of the highest density packing arrangement of molecules observed by STM in the high coverage image shown in Results and Discussion.

The single-crystal Pt(111) surfaces were cleaned by repeated cycles of Ar^+ (99.999% Messer) sputtering (1 keV, 5 μA) for 40 min and annealing at 1000 K. This process was followed by exposure to 5.5×10^{-8} Torr O_2 (Energas, 99.95%) for 25 min at 815 K. The sample was finally annealed to 1000 K. Surface cleanliness was confirmed by LEED, AES, or STM.

RESULTS AND DISCUSSION

Adsorption and Reactivity of Furfural on Pt(111). Figure 1a shows TPRS acquired after clean Pt(111) was

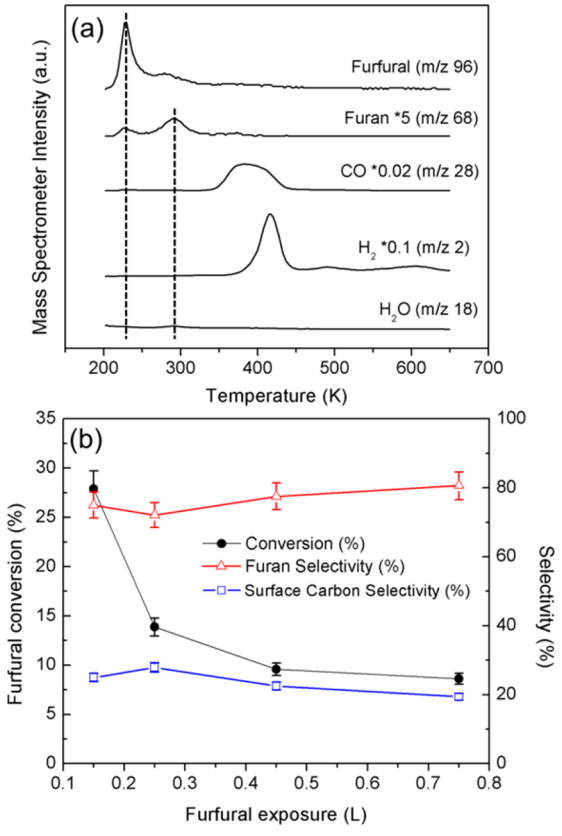

Figure 1. (a) Raw data showing the desorption products of furfural (0.15 L) on clean Pt(111). (b) Reactivity of the Pt(111) surface at varying furfural exposure.

exposed to 0.15 L furfural at 140 K. The evolved products were unreacted furfural (m/z 96) and reactively formed furan (m/z 68), CO (m/z 28), H_2 (m/z 2), and H_2O (m/z 18). A total of 72% of the adsorbed furfural desorbed intact (main peak at 227 K with a smaller more strongly bound feature at 280 K), whereas ~22% reacted to furan which desorbed at 291 K. The remainder formed surface carbon (see below), CO, and H_2. The small feature at 280 K in the desorption spectrum of furfural is associated with desorption from step edges of the crystal, and it does not increase significantly in intensity, as shown in Figure S1a. Note that furfural multilayer peaks on Pt(111) appear at 190 K (Figure S1a,b). Note that the 227 K peak in the furan desorption corresponds to furfural, which shares a m/z 68 fragment with furan. This m/z 68 fragment is sufficiently weak that we can be confident it is not the main contributor to the furan desorption at 291 K, and indeed the 280 K furfural peak is clearly offset in temperature from the former, confirming their different chemical origins. Carbon monoxide desorption due to furfural decarbonylation occurred at 384 K, coincident with the temperature for chemisorbed CO desorption over Pt(111), indicating the former's appearance was desorption-rate limited; hence, decarbonylation occurs below 384 K. H_2 desorption from furfural decomposition occurred at 415, 488, and 604 K. All three H_2 desorption peak temperatures are higher than that of chemisorbed H_2 over clean Pt(111); hence, their appearance was reaction-rate limited (see Figures 1a and S2a,b).

Liberation of surface atomic hydrogen from furfural decomposition (Figure 1a) does not lead to any self-hydrogenation products, presumably because the temperature for surface hydrogen formation is higher than the desorption temperature of furfuryl alcohol and methyl furan (Figure S3a,b). The hydrogen desorption peak area can be used to estimate the amount of residual carbon on Pt(111) following the temperature ramp as described in the Supporting Information. We estimate ~6% of the total adsorbed furfural adlayer remains as carbonaceous deposits. Figure 1b presents furfural total conversion and product selectivity as a function of exposure, revealing lower reactivity over crowded surfaces (conversion decreasing from 28% to 9%), while furan selectivity (and the amount of residual carbon) were coverage-independent. This fall in furfural conversion and subsequent plateau occurs around 0.45 L, coinciding with saturation of the furfural monolayer (Figure S1a). This saturation exposure is similar to that of 0.6 L reported by Shi and Vohs,[38] with higher exposure rapidly populating multilayers.

A microscopic view of furfural on Pt(111) at two different coverages was obtained by STM (Figures 2a–c and 3a–c).

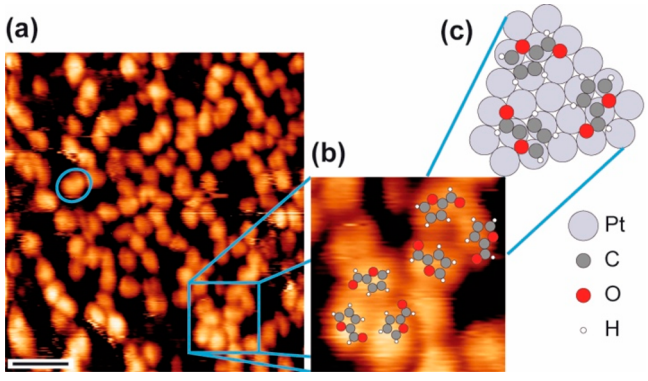

Figure 2. Submonolayer of furfural dosed to a Pt(111) surface kept at 95 K. (a) Overview STM image with a single furfural molecule indicated by the blue circle (T = 145 K, V_t = 1.28 V, I_t = 0.12 nA). The scale bar (black line) is 2 nm. (b) Expanded area from panel a, indicated by the blue square, overlaid with an atomistic scale model with furfural in a planar geometry. (c) Model of proposed hydrogen-bonded network on the Pt(111).

DOI: 10.1021/acs.jpcc.7b01744
J. Phys. Chem. C 2017, 121, 8490–8497

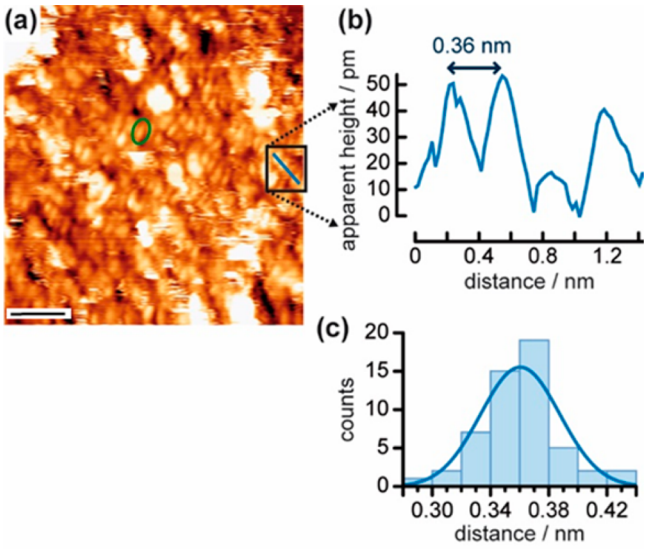

Figure 3. (a) STM image (T = 125 K, V_t = −1.58 V, I_t = 0.16 nA) with high furfural coverage dosed to a Pt(111) surface at 95 K. At coverages without any bare Pt, the line profile (b) across the line (highlighted by a square) indicated in panel a in the same color shows that the molecular features (example outlined in purple) are separated by ∼0.36 nm. The statistical separation of molecular features across the same direction is displayed in panel c. The scale bar (black line) in the STM image is 2 nm.

Figure 2a shows a representative image for ∼0.5 ML furfural, while Figure 3a that of a saturated furfural adlayer, which also features some multilayer patches. Individual furfural molecules (outlined in blue) are observed to self-assemble in Figure 2a, presumably because of attractive adsorbate−adsorbate interactions. Considering the optimal furfural adsorption geometry calculated by DFT,[36] we assign the bright protrusions in Figure 2a to individual furfural molecules. We further propose that this self-assembly is driven by weak hydrogen bonding between aromatic hydrogens and the carbonyl oxygen: aromatic−C−H···O═C−,[48] as shown in Figure 2b,c. At high coverage (Figure 3a), these bright features change appearance, forming narrow protrusions (example outlined in green). Such protrusions can be found to be as close as ∼0.36 nm apart (Figure 3b), much closer than the molecular footprint of a planar furfural molecule. The statistical distribution of the molecular features across the same direction is centered ∼0.36 nm (Figure 3c), which still cannot be accounted for with a model consisting of planar molecules. The packing density of furfural here is ∼3 molecules nm^{-2} as compared to a maximum density of ∼2 molecule nm^{-2} observed in the submonolayer surface (Figure 2a). This can be attributed to a change in the adsorption geometry toward a strongly tilted molecule, which is driven by the maximization of the number of molecules in contact with the metal surface.

At 245 K (above the main desorption peak of unreactive furfural), the STM reveals that at submonolayer coverages, some of the structures identified as single furfural molecules packing in the hydrogen-bonded networks are less discernible (Figure 4a). Smaller rounded protrusions enclosed within dotted blue circles whose dimensions are consistent with furan are now seen. At 265 K, above the temperature for furfural desorption and around the onset of that for reactively formed furan desorption, Figure 4b shows a decrease in the surface coverage of adsorbates.

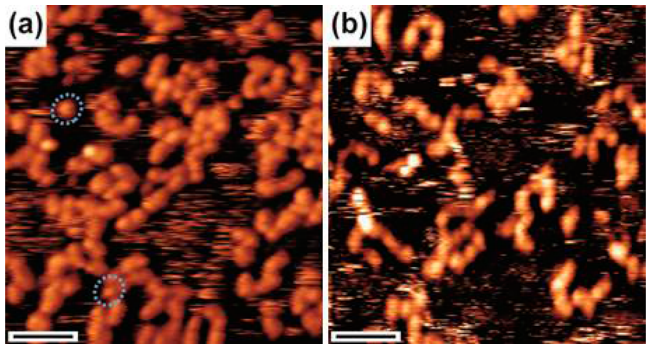

Figure 4. Temperature-dependent STM images of the molecular layer on Pt(111) after dosing ∼0.1 L furfural at 157 K. (a) After the the sample is heated to 245 K, molecular species consistent with furan, such as the ones in dotted circles, can be found (V_t = 1.06 V, I_t = 0.10 nA). (b) After further heating to 265 K, some furan molecules have desorbed, reducing the surface coverage (V_t = −0.45 V, I_t = 0.07 nA). The scale bar (black line) in the STM images is 2 nm.

Desorption Enthalpies for Furfural and Furan on Pt(111). Enthalpies of furfural and furan desorption from Pt(111) were determined from a Redhead analysis,[49] assuming a common pre-exponential factor of 10^{13} s^{-1} as widely adopted for organic adsorbates including phenol,[50] benzene,[51] and naphthalene.[52] The desorption enthalpy of chemisorbed furfural in the main desorption peak at 227 K was ∼56 kJ mol^{-1} (Figure 1a). This value appears to be close to the value calculated for the desorption of phenol (57 kJ mol^{-1}) and cyclopentane (58 kJ mol^{-1}) on similar Pt(111) surfaces.[50,53] Furfural desorption from Pd(111) occurs at a far higher temperature 365 K[39] and hence must be associated with a far greater activation barrier. Redhead analysis for reactively formed furan from flat-laying furan (Figure S4) reveals a desorption enthalpy of ∼73 kJ mol^{-1}, close to that of unsubstituted aromatics such as benzene with 68 kJ mol^{-1} over Pt(111).[51] DFT calculations for furfural on precious metals[39,54,55] have produced different values depending on the metal used and are sensitive to the inclusion of dispersive interactions.[54] A comparative study suggested that furfural adopts both C═C ring and C═O bonding motifs over Pd, whereas on Pt, adsorption occurs only through the C═C ring. The latter adsorption geometry is consistent with the ability of furfural to form the hydrogen-bonded networks described above. The stronger adsorption of furfural over Pd(111) versus Pt(111) undoubtedly underpins their different reactivity: furfural evolves furan (365 K), CO (460 K), and H_2 (330 and 410 K) over Pd(111) but also undergoes extensive ring decomposition leading to propylene (385 K).[37,39] In contrast, propylene was not observed over Pt(111) in this work.

Investigation and Quantification of Surface Carbon Product during Furfural Desorption from Pt(111). As discussed above, furfural adsorption over Pt results in carbon deposition, presenting a major technological drawback to utilizing Pt for large-scale furfural hydrogenation. Figure 5a,b shows consecutive TPRS profiles following a 0.25 L furfural exposure over Pt(111), without cleaning the surface each cycle. Figure 5a shows a 47% drop in furfural desorption intensity between the first and second cycle, with the amount of reactively formed hydrogen (Figure 5b) reduced by a similar amount (40%). However, between the second and third exposure, the furfural and hydrogen desorption intensities decrease by only a further 5% and 3%, respectively. These

DOI: 10.1021/acs.jpcc.7b01744
J. Phys. Chem. C 2017, 121, 8490−8497

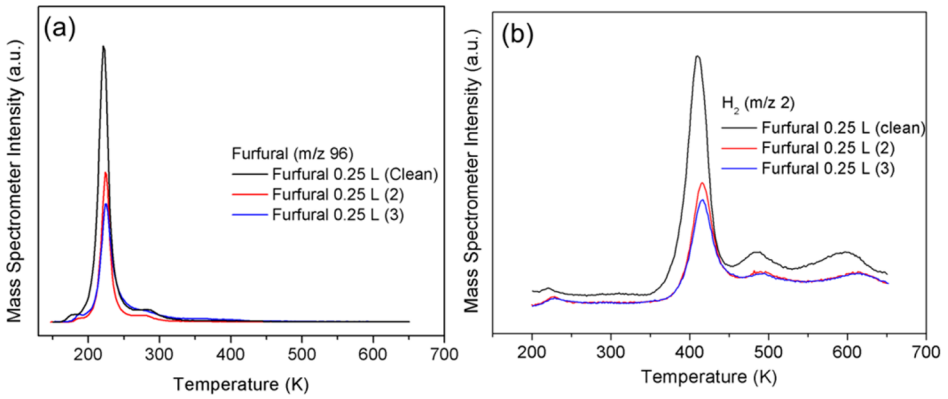

Figure 5. (a) Repeated exposure of furfural (0.25 L), followed by desorption, without surface cleaning in between cycles, showing diminished overall monolayer adsorption feature intensity at 222 K, indicating site blocking by carbon deposits. (b) Corresponding decrease in H_2 signal during adsorption−desorption cycles showing a decrease in reactive furfural due to carbonaceous deposits.

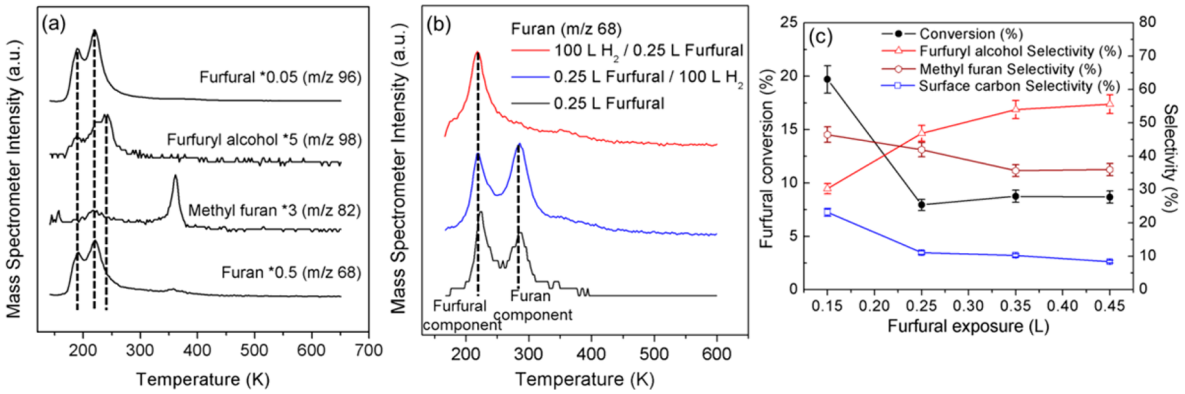

Figure 6. (a) TPRS for Pt(111) exposed to 100 L H_2 followed by 0.35 L furfural. (b) Reactively formed furan production from furfural over Pt(111) surfaces. (c) Furfural reactivity over Pt(111) pre-exposed to 100 L H_2 as a function of furfural exposure. Molecular adsorption was performed at 140 K in all cases.

observations demonstrate the number of available adsorption sites has decreased significantly, indicating the accumulation of significant (carbonaceous) residues. Furthermore, the initial decrease in furfural desorption of ∼47% between cycles one and two is significantly greater than the proportion of adsorbed furfural calculated to decompose to carbon (∼20% from Figure 1b). This suggests that any carbon deposits are likely uniformly distributed across the Pt(111) surface and hence block a large number of furfural adsorption sites. The formation of carbonaceous deposits from furfural is reportedly favored at 377−385 K over Pt catalysts during gas-phase hydrogenation,[20,56] comparable to the desorption temperature for reactively formed hydrogen (indicative of hydrocarbon decomposition) from furfural over Pt(111) shown in Figure 1a. High furan yields during liquid-phase hydrogenation of furfural over Pt nanoparticles is also reported around 343 K,[11] in good agreement with that for the desorption of reactively formed furan from Pt(111) in this work at 323 K. CO formed through furfural decarbonylation to furan may also be responsible for site-blocking and poisoning of Pt catalysts at temperatures below that necessary for desorption of the former.[11] Poisoning by carbon laydown typically requires catalyst reactivation (e.g., through calcination) and concomitant loss in metal surface area or changes in particle morphology and hence is often considered irreversible. In contrast, reversible CO poisoning may be mitigated by higher-temperature operation.

Furfural Hydrogenation on Pt(111). Hydrogen adsorption over clean Pt(111) was first studied by TPRS (Figure S2b) as a function of exposure. The desorption temperature of molecular hydrogen decreased with increasing H_2 exposure in accordance with the expected second-order kinetics reported by Gebhardt and Koel.[57] Hydrogen coverages were calculated according to the work of Ertl and co-workers wherein θH_{sat} was 0.8 ML.[58] Furfural and hydrogen were codosed, employing a H_2 exposure of 100 L (corresponding to ∼0.4 ML) to ensure vacant Pt sites were available for furfural adsorption.

Figure 6a shows data from TPRS of a 100 L H_2 exposure and subsequent 0.35 L furfural exposure at 140 K over Pt(111). Furfural exhibits a multilayer desorption peak at ∼190 K and a monolayer desorption at 227 K (Figures 6a and S1b). Similar total yields of reactively formed furfuryl alcohol (m/z 98) and methyl furan (m/z 82) were observed at 240 and 360 K, respectively; however, no furan desorption was observed (Figure 6b). Note that furan, furfuryl alcohol, and methyl furan desorptions contain a contribution from furfural (which also exhibits mass fragments at m/z 68, 82, and 98); however, the desorption temperatures of reactively formed furfuryl alcohol and methyl furan differ from that of furfural but are in close agreement to those observed from their respective molecularly adsorbed species (Figure S3a,b), indicating that their appearance is desorption-rate limited. Figure S2a shows the appearance of a low-temperature H_2 desorption peak around 306 K, indicated by an arrow, characteristic of the

DOI: 10.1021/acs.jpcc.7b01744
J. Phys. Chem. C 2017, 121, 8490−8497

recombinative desorption of molecularly adsorbed hydrogen (Figure S2b). Additional hydrogen desorption must arise from the coadsorbed furfural and indeed are identical to those observed following furfural adsorption over clean Pt(111) at 415, 488, and 604 K (Figure 1a). As noted in an earlier section, furfural autohydrogenation over Pt(111) does not occur (Figure 1a); however, the observation of furfuryl alcohol in the presence of coadsorbed hydrogen indicates that furfural hydrogenation is possible over Pt(111) under UHV, provided that a high concentration of hydrogen adatoms is available at a relatively low surface temperature.

Reversing the dosing sequence, such that Pt(111) was first exposed to 0.25 L furfural followed by 100 L H_2, suppressed hydrogenation pathways to both furfuryl alcohol and methyl furan, affording a conversion and selectivity similar to that seen over clean Pt(111). The main product observed is furan desorbing at 291 K (Figure 6b). Figure 6c shows furfural conversion and selectivity as a function of furfural exposure over Pt(111) precovered with 100 L H_2.The results are in excellent agreement with the reaction pathways proposed in Scheme 1. At low furfural exposures (corresponding to a high ratio of surface H(a):furfural), the stepwise hydrogenation of furfural to furfuryl alcohol, and its subsequent HDO to methyl furan, is favored. At high furfural exposures (a low surface H(a):furfural ratio), insufficient surface hydrogen is available to further hydrogenate reactively formed furfuryl alcohol, which hence becomes the dominant product; however, in the latter scenario, more furfural desorbs molecularly.

The preceding insight enables us to predict the selectivity to furfuryl alcohol during furfural hydrogenation (Figure 7);

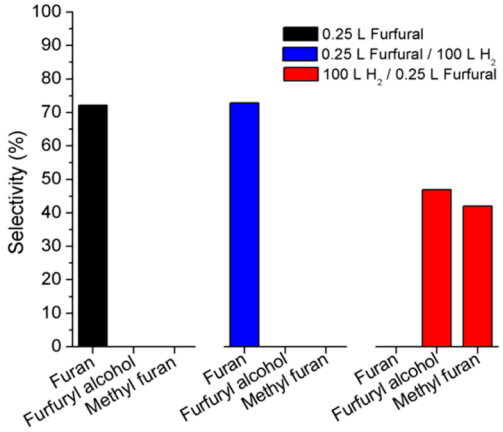

Figure 7. Gas-phase selectivities to molecular products for furfural with and without H_2 and for different orders of exposure to the two reactants.

higher surface hydrogen concentrations encountered in gas-phase furfural hydrogenation are expected to favor methyl furan relative to furfuryl alcohol, whereas the latter should be favored in the liquid phase. This is precisely as reported in the literature.[11,12,20,59]

CONCLUSIONS

The hydrogenation of furfural on Pt(111) was found to be highly sensitive to the conditions, in particular, surface crowding and associated changes in the adsorption geometry, used to carry out the catalytic reaction. On clean Pt(111), furfural adopts a planar motif at low coverages and a more tilted geometry as the coverage is increased. The extent of decarbonylation to furan was found to depend strongly on the coverage (and therefore adsorption geometry): at low coverage, the planar motif results in a much greater conversion to furan than occurs in the higher-coverage tilted molecules. The formation of surface carbon and possible consequences for practical catalyst deactivation processes have also been investigated and discussed.

Control of the furfural coverage on the surface is critical to the reaction selectivity, with hydrogenation and hydrogenolysis being possible at higher coverages. A strong correlation between the reactivity of the Pt(111) surface with that of Pt dispersed systems was observed, which enables the prediction of the activity and selectivity of Pt-based catalysts under practical conditions in the liquid and the gas phase. The order in which the surface encounters hydrogen and furfural is critically important. When furfural encounters a bare surface, it hinders the subsequent dissociative chemisorption of hydrogen and resulting hydrogenation activity. In contrast, when furfural encounters preadsorbed atomic hydrogen, furfuryl alcohol and methyl furan are produced; the former is a product of direct furfural hydrogenation, and the latter is a secondary product arising from the HDO of furfuryl alcohol (requiring a high ratio of surface H(a):furfural). At a low surface H(a):furfural ratio, insufficient surface hydrogen is available to further hydrogenate reactively formed furfuryl alcohol, which hence becomes the dominant product. Our results indicate that control over the furfural adsorption geometry, and surface hydrogen concentration, are key considerations for the design and operation of practical Pt catalysts for this important bioeconomy transformation.

ASSOCIATED CONTENT

Supporting Information

The Supporting Information is available free of charge on the ACS Publications website at DOI: 10.1021/acs.jpcc.7b01744.

Additional TPR spectra as well as the protocols used for calculating reagent conversion and product selectivities (PDF)

AUTHOR INFORMATION

Corresponding Author

*E-mail: g.kyriakou@aston.ac.uk.

ORCID

Martin J. Taylor: 0000-0002-8810-8942
Anthoula C. Papageorgiou: 0000-0003-1054-0097
Simon K. Beaumont: 0000-0002-1973-9783
Karen Wilson: 0000-0003-4873-708X
Adam F. Lee: 0000-0002-2153-1391
Georgios Kyriakou: 0000-0001-6295-844X

Notes

The authors declare no competing financial interest.

ACKNOWLEDGMENTS

M.J.T. thanks Aston University for a Ph.D. studentship; K.W. thanks the EPSRC for funding under EP/K014676/1 and EP/K014749/1; L.J. acknowledges funding of the China Scholarship Council (CSC). This work was supported by the European Research Council Advanced Grant MolArt (No. 247299). S.K.B. thanks both the Durham University Addison Wheeler scheme and the Leverhulme Trust's Early Career Fellowship

DOI: 10.1021/acs.jpcc.7b01744
J. Phys. Chem. C 2017, 121, 8490−8497

scheme. G.K. acknowledges funding from the Royal Society and EPSRC (EP/M005186/2)

REFERENCES

(1) Yan, K.; Wu, G.; Lafleur, T.; Jarvis, C. Production, properties and catalytic hydrogenation of furfural to fuel additives and value-added chemicals. *Renewable Sustainable Energy Rev.* **2014**, *38*, 663−676.

(2) Mandalika, A.; Qin, L.; Sato, T. K.; Runge, T. Integrated biorefinery model based on production of furans using open-ended high yield processes. *Green Chem.* **2014**, *16*, 2480−2489.

(3) Gallezot, P. Conversion of biomass to selected chemical products. *Chem. Soc. Rev.* **2012**, *41*, 1538−1558.

(4) Climent, M. J.; Corma, A.; Iborra, S. Conversion of biomass platform molecules into fuel additives and liquid hydrocarbon fuels. *Green Chem.* **2014**, *16*, 516−547.

(5) Elliott, D. C.; Hart, T. R. Catalytic hydroprocessing of chemical models for bio-oil. *Energy Fuels* **2009**, *23*, 631−637.

(6) Besson, M.; Gallezot, P.; Pinel, C. Conversion of biomass into chemicals over metal Catalysts. *Chem. Rev.* **2014**, *114*, 1827−1870.

(7) Sharma, R. V.; Das, U.; Sammynaiken, R.; Dalai, A. K. Liquid phase chemo-selective catalytic hydrogenation of furfural to furfuryl alcohol. *Appl. Catal., A* **2013**, *454*, 127−136.

(8) Nakagawa, Y.; Tomishige, K. Production of 1,5-pentanediol from biomass via furfural and tetrahydrofurfuryl alcohol. *Catal. Today* **2012**, *195*, 136−143.

(9) Iqbal, S.; Liu, X.; Aldosari, O. F.; Miedziak, P. J.; Edwards, J. K.; Brett, G. L.; Akram, A.; King, G. M.; Davies, T. E.; Morgan, D. J.; et al. Conversion of furfuryl alcohol into 2-methylfuran at room temperature using Pd/TiO_2 catalyst. *Catal. Sci. Technol.* **2014**, *4*, 2280−2286.

(10) Aldosari, O. F.; Iqbal, S.; Miedziak, P. J.; Brett, G. L.; Jones, D. R.; Liu, X.; Edwards, J. K.; Morgan, D. J.; Knight, D. K.; Hutchings, G. J. Pd-Ru/TiO_2 catalyst - an active and selective catalyst for furfural hydrogenation. *Catal. Sci. Technol.* **2016**, *6*, 234−242.

(11) Taylor, M. J.; Durndell, L. J.; Isaacs, M. A.; Parlett, C. M. A.; Wilson, K.; Lee, A. F.; Kyriakou, G. Highly selective hydrogenation of furfural over supported Pt nanoparticles under mild conditions. *Appl. Catal., B* **2016**, *180*, 580−585.

(12) Chen, X.; Zhang, L.; Zhang, B.; Guo, X.; Mu, X. Highly selective hydrogenation of furfural to furfuryl alcohol over Pt nanoparticles supported on g-C_3N_4 nanosheets catalysts in water. *Sci. Rep.* **2016**, *6*, 28558.

(13) Bhogeswararao, S.; Srinivas, D. Catalytic conversion of furfural to industrial chemicals over supported Pt and Pd catalysts. *J. Catal.* **2015**, *327*, 65−77.

(14) Merlo, A. B.; Vetere, V.; Ruggera, J. F.; Casella, M. L. Bimetallic PtSn catalyst for the selective hydrogenation of furfural to furfuryl alcohol in liquid-phase. *Catal. Commun.* **2009**, *10*, 1665−1669.

(15) Merlo, A. B.; Vetere, V.; Ramallo-López, J. M.; Requejo, F. G.; Casella, M. L. Liquid-phase furfural hydrogenation employing silica-supported PtSn and PtGe catalysts prepared using surface organometallic chemistry on metals techniques. *React. Kinet., Mech. Catal.* **2011**, *104*, 467−482.

(16) Egeblad, K.; Rass-Hansen, J.; Marsden, C.; Taarning, E.; Hviid Christensen, C. Heterogeneous catalysis for production of value-added chemicals from biomass. *Catalysis* **2009**, *21*, 13−50.

(17) Gowda, A. S.; Parkin, S.; Ladipo, F. T. Hydrogenation and hydrogenolysis of furfural and furfuryl alcohol catalyzed by ruthenium-(II) bis(diimine) complexes. *Appl. Organomet. Chem.* **2012**, *26*, 86−93.

(18) Wojcik, B. H. Catalytic hydrogenation of furan compounds. *Ind. Eng. Chem.* **1948**, *40*, 210−216.

(19) Nagaraja, B. M.; Siva Kumar, V.; Shasikala, V.; Padmasri, A. H.; Sreedhar, B.; David Raju, B.; Rama Rao, K. S. A highly efficient Cu/MgO catalyst for vapour phase hydrogenation of furfural to furfuryl alcohol. *Catal. Commun.* **2003**, *4*, 287−293.

(20) Pushkarev, V. V.; Musselwhite, N.; An, K.; Alayoglu, S.; Somorjai, G. A. High structure sensitivity of vapor-phase furfural decarbonylation/hydrogenation reaction network as a function of size and shape of Pt nanoparticles. *Nano Lett.* **2012**, *12*, 5196−5201.

(21) Pang, S. H.; Schoenbaum, C. A.; Schwartz, D. K.; Medlin, W. J. Effects of thiol modifiers on the kinetics of furfural hydrogenation over Pd catalysts. *ACS Catal.* **2014**, *4*, 3123−3131.

(22) Villaverde, M. M.; Bertero, N. M.; Garetto, T. F.; Marchi, A. J. Selective liquid-phase hydrogenation of furfural to furfuryl alcohol over Cu-based catalysts. *Catal. Today* **2013**, *213*, 87−92.

(23) Audemar, M.; Ciotonea, C.; De Oliveira Vigier, K.; Royer, S.; Ungureanu, A.; Dragoi, B.; Dumitriu, E.; Jerome, F. Selective hydrogenation of furfural to furfuryl alcohol in the presence of a recyclable cobalt/SBA-15 catalyst. *ChemSusChem* **2015**, *8* (11), 1885−1891.

(24) Sitthisa, S.; An, W.; Resasco, D. E. Selective conversion of furfural to methylfuran over silica-supported NiFe bimetallic catalysts. *J. Catal.* **2011**, *284*, 90−101.

(25) Kijeński, J.; Winiarek, P.; Paryjczak, T. Platinum deposited on monolayer supports in selective hydrogenation of furfural to furfuryl alcohol. *Appl. Catal., A* **2002**, *233*, 171−182.

(26) Vargas-Hernández, D.; Rubio-Caballero, J. M.; Santamaría-González, J.; Moreno-Tost, R.; Mérida-Robles, J. M.; Pérez-Cruz, M. A.; Jiménez-López, A.; Hernández-Huesca, R.; Maireles-Torres, P. Furfuryl alcohol from furfural hydrogenation over copper supported on SBA-15 silica catalysts. *J. Mol. Catal. A: Chem.* **2014**, *383*−*384*, 106−113.

(27) Mironenko, R. M.; Belskaya, O. B.; Gulyaeva, T. I.; Nizovskii, A. I.; Kalinkin, A. V.; Bukhtiyarov, V. I.; Lavrenov, A. V.; Likholobov, V. A. Effect of the nature of carbon support on the formation of active sites in Pd/C and Ru/C catalysts for hydrogenation of furfural. *Catal. Today* **2015**, *249*, 145−152.

(28) Reyes, P.; Salinas, D.; Campos, C.; Oportus, M. Selective hydrogenation of furfural on Ir/TiO_2 catalysts. *Quim. Nova* **2010**, *33*, 777−780.

(29) Vetere, V.; Merlo, A. B.; Ruggera, J. F.; Casella, M. L. Transition metal-mased bimetallic catalysts for the chemoselective hydrogenation of furfuraldehyde. *J. Braz. Chem. Soc.* **2010**, *21*, 914−920.

(30) Mattson, B.; Foster, W.; Greimann, J.; Hoette, T.; Le, N.; Mirich, A.; Wankum, S.; Cabri, A.; Reichenbacher, C.; Schwanke, E. Heterogeneous catalysis: The Horiuti−Polanyi mechanism and alkene hydrogenation. *J. Chem. Educ.* **2013**, *90*, 613−619.

(31) Nakagawa, Y.; Tamura, M.; Tomishige, K. Catalytic conversions of furfural to pentanediols. *Catal. Surv. Asia* **2015**, *19*, 249−256.

(32) Shi, Y.; Zhu, Y.; Yang, Y.; Li, Y. W.; Jiao, H. Exploring furfural catalytic conversion on Cu(111) from computation. *ACS Catal.* **2015**, *5*, 4020−4032.

(33) Vorotnikov, V.; Mpourmpakis, G.; Vlachos, D. G. DFT study of furfural conversion to furan, furfuryl alcohol, and 2-methylfuran on Pd(111). *ACS Catal.* **2012**, *2*, 2496−2504.

(34) Wang, S.; Vorotnikov, V.; Sutton, J. E.; Vlachos, D. G. Brønsted-Evans-Polanyi and transition state scaling relations of furan derivatives on Pd(111) and their relation to those of small molecules. *ACS Catal.* **2014**, *4*, 604−612.

(35) Wang, S.; Vorotnikov, V.; Vlachos, D. G. Coverage-induced conformational effects on activity and selectivity: hydrogenation and decarbonylation of furfural on Pd(111). *ACS Catal.* **2015**, *5*, 104−112.

(36) Liu, B.; Cheng, L.; Curtiss, L.; Greeley, J. Effects of van der waals density functional corrections on trends in furfural adsorption and hydrogenation on close-packed transition metal surfaces. *Surf. Sci.* **2014**, *622*, 51−59.

(37) Williams, R.; Pang, S. H.; Medlin, J. W. Ring opening and oxidation pathways of furanic oxygenates on oxygen-precovered Pd(111). *J. Phys. Chem. C* **2014**, *118*, 27933−27943.

(38) Shi, D.; Vohs, J. M. Deoxygenation of biomass-derived oxygenates: reaction of furfural on Zn-modified Pt(111). *ACS Catal.* **2015**, *5*, 2177−2183.

(39) Pang, S. H.; Medlin, J. W. Adsorption and reaction of furfural and furfuryl alcohol on Pd(111): unique reaction pathways for multifunctional reagents. *ACS Catal.* **2011**, *1*, 1272−1283.

(40) Wilson, K. E.; Baddeley, C. J. Understanding the surface chemistry of enantioselective heterogeneous reactions influence of modification variables on the interaction of methylacetoacetate with

DOI: 10.1021/acs.jpcc.7b01744
J. Phys. Chem. C 2017, 121, 8490−8497

(S)-aspartic acid modified Ni(111). *J. Phys. Chem. C* **2009**, *113*, 10706−10711.
(41) Yao, Y.; Zaera, F. Adsorption and thermal chemistry of formic acid on clean and oxygen-predosed Cu(110) single-crystal surfaces revisited. *Surf. Sci.* **2016**, *646*, 37−44.
(42) Goubert, G.; Groves, M. N.; Dong, Y.; Lemay, J.-C.; McBreen, P. H.; Hammer, B. Isolating a reaction intermediate in the hydrogenation of 2,2,2-trifluoroacetophenone on Pt(111). *J. Phys. Chem. C* **2015**, *119*, 7319−7326.
(43) Lawton, T. J.; Pushkarev, V.; Wei, D.; Lucci, F. R.; Sholl, D. S.; Gellman, A. J.; Sykes, E. C. H. Long range chiral imprinting of Cu(110) by tartaric acid. *J. Phys. Chem. C* **2013**, *117*, 22290−22297.
(44) Marcinkowski, M. D.; Liu, J.; Murphy, C. J.; Liriano, M. L.; Wasio, N. A.; Lucci, F. R.; Flytzani-Stephanopoulos, M.; Sykes, E. C. H. Selective formic acid dehydrogenation on Pt-Cu single-atom alloys. *ACS Catal.* **2017**, *7*, 413−420.
(45) Stacchiola, D.; Calaza, F.; Burkholder, L.; Tysoe, W. T. Vinyl acetate formation by the reaction of ethylene with acetate species on oxygen-covered Pd(111). *J. Am. Chem. Soc.* **2004**, *126*, 15384−15385.
(46) Ormerod, R. M.; Baddeley, C. J.; Hardacre, C.; Lambert, R. M. Chemisorption and reactivity of furan on Pd (111). *Surf. Sci.* **1996**, *360*, 1−9.
(47) Horcas, I.; Fernández, R.; Gómez-Rodríguez, J. M.; Colchero, J.; Gómez-Herrero, J.; Baro, A. M. WSXM: A software for scanning probe microscopy and a tool for nanotechnology. *Rev. Sci. Instrum.* **2007**, *78*, 013705−013712.
(48) Lavoie, S.; McBreen, P. H. Evidence for C−H···O═C bonding in coadsorbed aromatic−carbonyl systems on Pt(111). *J. Phys. Chem. B* **2005**, *109*, 11986−11990.
(49) Redhead, P. A. Thermal desorption of gases. *Vacuum* **1962**, *12* (4), 203−211.
(50) Ihm, H.; White, J. M. Stepwise dissociation of thermally activated phenol on Pt(111). *J. Phys. Chem. B* **2000**, *104*, 6202−6211.
(51) Ihm, H.; Ajo, H. M.; Gottfried, J. M.; Bera, P.; Campbell, C. T. Calorimetric measurement of the heat of adsorption of benzene on Pt(111). *J. Phys. Chem. B* **2004**, *108*, 14627−14633.
(52) Gottfried, J. M.; Vestergaard, E. K.; Bera, P.; Campbell, C. T. Heat of adsorption of naphthalene on Pt(111) measured by adsorption calorimetry. *J. Phys. Chem. B* **2006**, *110*, 17539−17545.
(53) Avery, N. R. Adsorption and reactivity of cyclopentane on Pt(111). *Surf. Sci.* **1985**, *163*, 357−368.
(54) Liu, B.; Cheng, L.; Curtiss, L.; Greeley, J. Effects of van der waals density functional corrections on trends in furfural adsorption and hydrogenation on close-packed transition metal surfaces. *Surf. Sci.* **2014**, *622*, 51−59.
(55) Rogers, S. M.; Catlow, C. R. A.; Chan-Thaw, C. E.; Chutia, A.; Jian, N.; Palmer, R. E.; Perdjon, M.; Thetford, A.; Dimitratos, N.; Villa, A.; et al. Tandem site and size controlled Pd nanoparticles for the directed hydrogenation of furfural. *ACS Catal.* **2017**, *7*, 2266−2274.
(56) Baker, L. R.; Kennedy, G.; Van Spronsen, M.; Hervier, A.; Cai, X.; Chen, S.; Wang, L.-W.; Somorjai, G. A. Furfuraldehyde hydrogenation on titanium oxide-supported platinum nanoparticles studied by sum frequency generation vibrational spectroscopy: acid-base catalysis explains the molecular origin of strong metal-support interactions. *J. Am. Chem. Soc.* **2012**, *134*, 14208−14216.
(57) Gebhard, S. C.; Koel, B. E. Influence of potassium on the adsorption of hydrogen on platinum(111). *J. Phys. Chem.* **1992**, *96*, 7056−7063.
(58) Christmann, K.; Ertl, G.; Pignet, T. Adsorption of hydrogen on a Pt(111) surface. *Surf. Sci.* **1976**, *54*, 365−392.
(59) An, K.; Musselwhite, N.; Kennedy, G.; Pushkarev, V. V.; Baker, L. R.; Somorjai, G. A. Preparation of mesoporous oxides and their support effects on Pt nanoparticle catalysts in catalytic hydrogenation of furfural. *J. Colloid Interface Sci.* **2013**, *392* (392), 122−128.

DOI: 10.1021/acs.jpcc.7b01744
J. Phys. Chem. C 2017, 121, 8490−8497